Materials Today: Proceedings 25 (2020) 88–92

Contents lists available at ScienceDirect

Materials Today: Proceedings

journal homepage: www.elsevier.com/locate/matpr

Nanoscale thermal transport and elastic properties of lithiated amorphous Si thin films

Azat Abdullaev [a,*], Aliya Mukanova [b,*], Talgat Yakupov [a], Almagul Mentbayeva [b], Zhumabay Bakenov [b], Zhandos Utegulov [a]

[a] Department of Physics, School of Sciences and Humanities, Nazarbayev University, Nur-Sultan 010000, Kazakhstan
[b] Department of Chemical and Materials Engineering, School of Engineering and Digital Sciences, National Laboratory Astana, Nazarbayev University, Nur-Sultan 010000, Kazakhstan

ARTICLE INFO

Article history:
Received 23 August 2019
Received in revised form 27 October 2019
Accepted 25 November 2019
Available online 16 January 2020

Keywords:
Amorphous silicon
Thin film
Lithium-ion batteries
Thermal transport
Elastic properties
Lithiation

ABSTRACT

Silicon is the heart of modern electronics and due to it is high theoretical storage capacity it also attracted much attention as a possible anode material for the next generation Li-ion batteries. Heat conduction is one of the major properties in the development of Li-ion batteries for energy conversion systems and it is of paramount importance to have comprehensive understanding of heat dissipation on the scale of electrochemical storage device. In this work we report *ex-situ* study of nanoscale thermal transport and elastic properties of lithiated amorphous Si (a-Si) anode films using picosecond time-domain thermoreflectance (TDTR). Radio frequency (*rf*) magnetron sputtering was used to deposit a ~330 nm thick a-Si films on glass substrate. Near-surface nanoscale thermal transport measurements show 40% increase in thermal conductivity of a-Si upon electrochemical lithiation reaching up to 2.2 $W m^{-1}K^{-1}$. This sizeable increase might be due to Li^+ ion-mediated heat conduction during lithiation process. The standard deviation of measured thermal conductivity was slightly higher likely due to inhomogeneous lateral and cross-plane Li^+ ions distribution in the sub-surface film region. Nanosecond laser pulsed induced surface acoustic waves (SAWs) measurements showed the decrease in Young's modulus after lithiation on nanometre scale, which is attributed to volumetric expansion of Si upon Li^+ ions insertion.

Selection and peer-review under responsibility of the scientific committee of the 7th International Conference on Nanomaterials and Advanced Energy Storage Systems.

1. Introduction

Rechargeable Li-ion batteries (LIBs) have found a wide range of applications as a prevailing source for portable electronic devices and they are promising candidates as an energy source in the future electrical vehicles and energy storage systems for alternative energy applications [1,2]. Currently plenty of research has been devoted to improving power and cycle lifespan of materials employed in Li-ion batteries. However, the safety issue is still unsolved in these devices and it is mostly related with overheating problem [3]. Electrical conduction properties in these systems are strongly affected by thermal transport and mechanical properties during electrochemical cycling. During the electrochemical charging and discharging processes the heat is generated when the current flows through the internal resistance of the battery [4]. This overheating will affect the performance, lifespan and safety of the battery [5]. If the overheating, which leads to poor heat dissipation, is not properly managed, serious safety problems might take place and even lead to battery explosion [3]. Therefore, thermal management in these systems is very important to ensure operation safety and to control the electrical properties of these storage devices.

One of the key thermodynamic properties of material is its thermal conductivity which is strongly dependent on the direction of heat propagation in anisotropic systems. Several experimental results have been reported on thermal conductivity measurements of Li-ion materials including electrodes [6–8], electrolyte [9] and separators [10–11] along the in-plane and cross-plane directions. Different thermal property measurement techniques were employed such as time domain thermoreflectance (TDTR) [8], heat flowmeter [9], DC heating method [10] and laser flash method [7].

In this work we investigated the variation of cross-plane thermal conductivity of lithiated and non-lithiated amorphous Si

* Corresponding authors. Tel.: +7172-709046 (A. Abdullaev), Tel.: +7172-706197 (A. Mukanova).
E-mail addresses: azat.abdullaev@nu.edu.kz (A. Abdullaev), aliya.mukanova@nu.edu.kz (A. Mukanova).

https://doi.org/10.1016/j.matpr.2019.11.333
2214-7853/
Selection and peer-review under responsibility of the scientific committee of the 7th International Conference on Nanomaterials and Advanced Energy Storage Systems.

(a-Si) thin films using TDTR technique. The main advantage of TDTR is ability to probe thermal properties variations on subsurface nanometer depth scale where electrochemical and thermal processes couple to each other.

Silicon is a very attractive anode material in LIBs because of potentially large achievable electrical capacity of 3700 $mAhg^{-1}$ [12] that is ten times more than that for graphitic carbon, which is conventionally used as an anode material in LIBs. Moreover, Si is relatively abundant, low cost and non-toxic material [13]. Specifically, a-Si is known to be more desirable for anode material than crystalline Si (c-Si) because the former can experience uniform lithiation avoiding the extensive formation of particle cracks [14,15] while the latter displays thin film thermal anisotropy and strong dependence on phonon mean free path [16]. Despite numerous studies on improvement of Si anode, the poor cycling, material degradation, structural and morphological changes remain major issues for the commercialization of Si-based anodes [17,18]. Besides, thermal overheating can also accelerate degradation process of the Si anode material. To the best of our knowledge, there have been no prior studies of thermal transport and mechanical properties variation in a-Si films during lithiation.

Although silicon exhibits great potential, this material suffers from enormous volumetric change during the electrochemical cycling/recycling processes, which in turn leads to alterations in mechanical and electrical properties. The volume deformation can be on the order of 300% [19] forming cracks and causing failure of electrodes and vanishing of electrical capacity. Different theoretical models have been developed to explain variation in elastic properties of lithiated and delithiated Si electrodes [20,21] including density functional theory (DFT) studies [22] demonstrating elastic softening of amorphous a-Si and crystalline c-Si electrodes. Studies also show the importance of assessment of Young's modulus in stress evolution of electrodes as a function of Li-ion concentration [23]. Therefore it is also crucial to investigate mechanical strength variation in lithiated Si films in addition to their thermal transport and electrical properties. In this work we employ nanosecond laser generated surface acoustic waves (SAWs) to measure elastic properties of lithiated samples.

2. Experimental part

2.1. Material fabrication and characterization

The ~330 nm thick silicon thin films were deposited on the top of thin copper layer (60 nm) which was used as a current collector on a glass substrate using RF magnetron sputtering system (LAB-18 from Kurt J. Lesker Company) using the *n*-type Si (<0.1 Ω•cm, 99.999%) and Cu (99.99%) targets. The total thickness of Cu and Si film was measured using profiling approach by atomic force microscopy (AFM, C3M SmartSPM-1000 from AIST-HT). Fig. 1a shows the AFM image of Si thin film, where it could be seen that sample surface has roughness <20 nm. Scanning electron microscopic (SEM, Crossbeam 540 from Zeiss) imaging enabled investigating the morphology of the particle. From Fig. 1b, the spherical shape of the Si particles with the average size lower than 100 nm can be observed, besides each such particle is a cluster built by many smaller particles. According to transmission electron microscopy (TEM, JEM-2100 from JEOL Ltd.) shown in Fig. 1c, the obtained Si thin film does not exhibit the crystal patterns indicating its complete amorphous phase The electrochemical lithiation of studied films was performed in the beaker cell (see Fig. 1d) with lithium metal as an opposite electrode and source of Li^+ ions, lithium hexafluorophosphate (LPF_6) liquid electrolyte in the solution of ethylene, diethyl carbonate and ethyl methyl carbonates

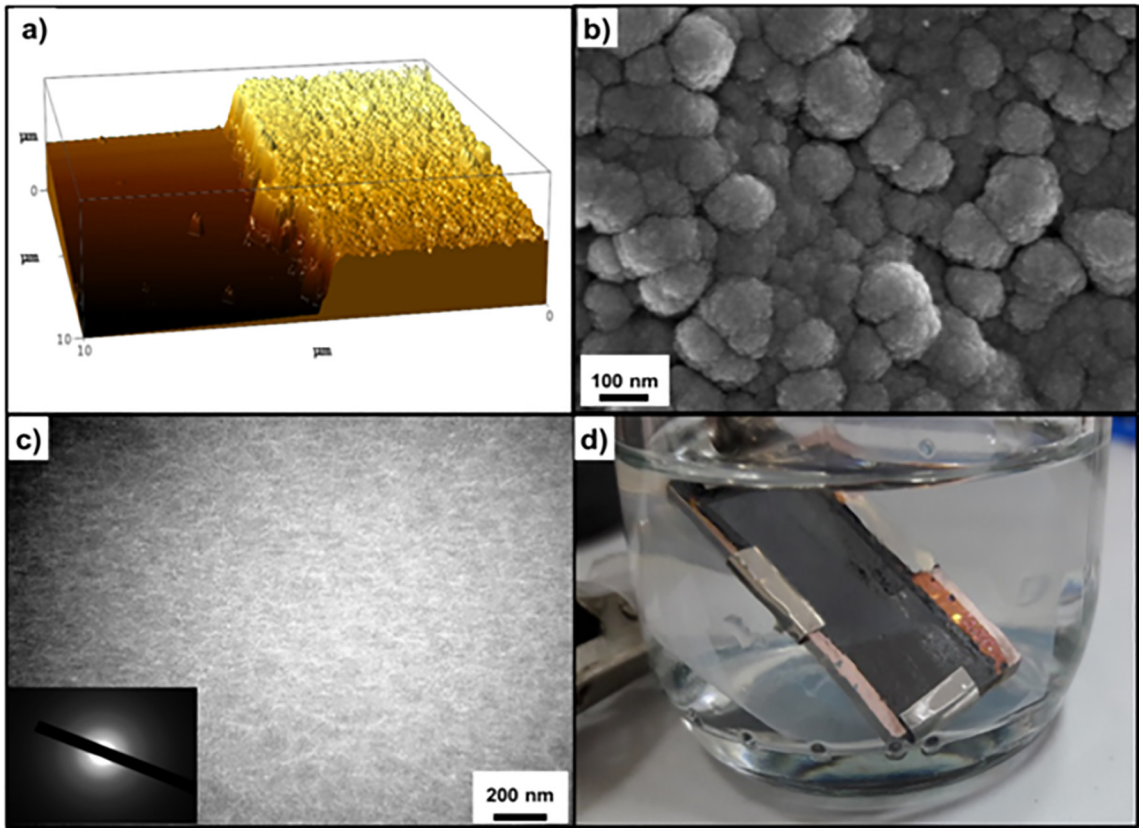

Fig. 1. (a) AFM image of pristine Si film, (b) SEM image of Si particles, (c) TEM pattern of pristine Si thin film and (d) beaker cell with Si anode immersed into electrolyte.

(EC:DC:EMC = 1:1:1, by vol.). The lithiation was performed galvanostatically on battery tester BT-2000 (Arbin Instruments) using a constant current of 25 μA up to a lower cut-off potential of 0.3 V and 0.05 V which is enough for the formation of higher lithiated phases of Li_xSi alloys [24].

2.2. Experimental setup

A picosecond TDTR setup was used to study heat transfer in non-lithiated and lithiated silicon anode thin film samples. This technique is a non-contact ultrafast optical pump–probe method that enables measuring thermal conductivity of thin films, single- and multi-layered structures and near-surface regions of bulk materials with nanoscale depth resolution and thermal conductance across dissimilar interfaces [25,26,33]. The schematic diagram of our constructed TDTR setup is shown in Fig. 2. A mode-locked Ti:sapphire laser (Spectra Physics, Tsunami) producing 80 fs pulses of 782 nm laser radiation at repetition rate of 80 MHz is split into two paths: one of which is a "pump" beam, depositing heat into the sample, while the second one is a "probe" beam which measures optical reflectivity from the sample under thermal excursions. The reflected probe is directed to the photodetector employing lock-in amplifier synchronized to the pump beam's modulation frequency set by the electro-optic modulator and function generator.

Fig. 3 shows obtained experimental data of non-lithiated (black line) and lithiated (red line) silicon. This is typical thermoreflectance signal which displays the change in optical reflectivity with temperature. The inset of Fig. 3 shows zoomed transient region up to 80 ps, which demonstrates picosecond acoustic echo to determine the thickness of Al layer. When pump beam heats the Al it leads to thermal stress which in turn excites acoustical waves inside the metal. By knowing the arrival time of these waves and speed of sound of Al layer, we can calculate its thickness.

Sample surface rapidly heats in about one picosecond, and then slowly cools down in a few nanoseconds. Immediately after the thermoreflectance signal maximum is reached, the fluctuations occur due to the reflection of acoustic waves generated by the pump laser from the interface ~60 nm thick heat-transducing aluminium thin film and underlying sample material itself, i.e. silicon anode film as shown in Fig. 3. The first 3 ns of thermoreflectance signal is recorded, due to motorized time delay set between the pump and probe beams during the experiment. Thus, the intensity of the probe laser beam reflected from the sample surface is measured several picoseconds before heating, at the very beginning of heating (at t = 0) and during the transient decay, during the first 3 ns. The transient decay of the change in thermoreflectance is then fitted to a theoretical thermal diffusion model to accurately determine thermal transport properties of the material under study [25].

The nanosecond laser pulse-generated SAWs with their piezo sensor detection (LaWave system Fraunhofer IWS) was employed to measure the elastic properties of nanoscale-thick unlithiated and lithiated thin films of amorphous silicon anodes on crystalline silicon substrates. The purpose of the measurements was to determine the effect of lithiation on the elastic properties of amorphous silicon anodes. The propagation of acoustic waves in layered media results in the so-called SAW phonon dispersion, i.e. ultrasonic waves with different frequencies travel with different phase velocities [27]. Thus, the shape of the measured surface acoustic signal changes with increasing distance between the measurement point and the source of SAW excitation.

Nanosecond pulsed laser with repetition frequency of 10 Hz, pulse duration of 3 ns, the laser wavelength of 353 nm was used

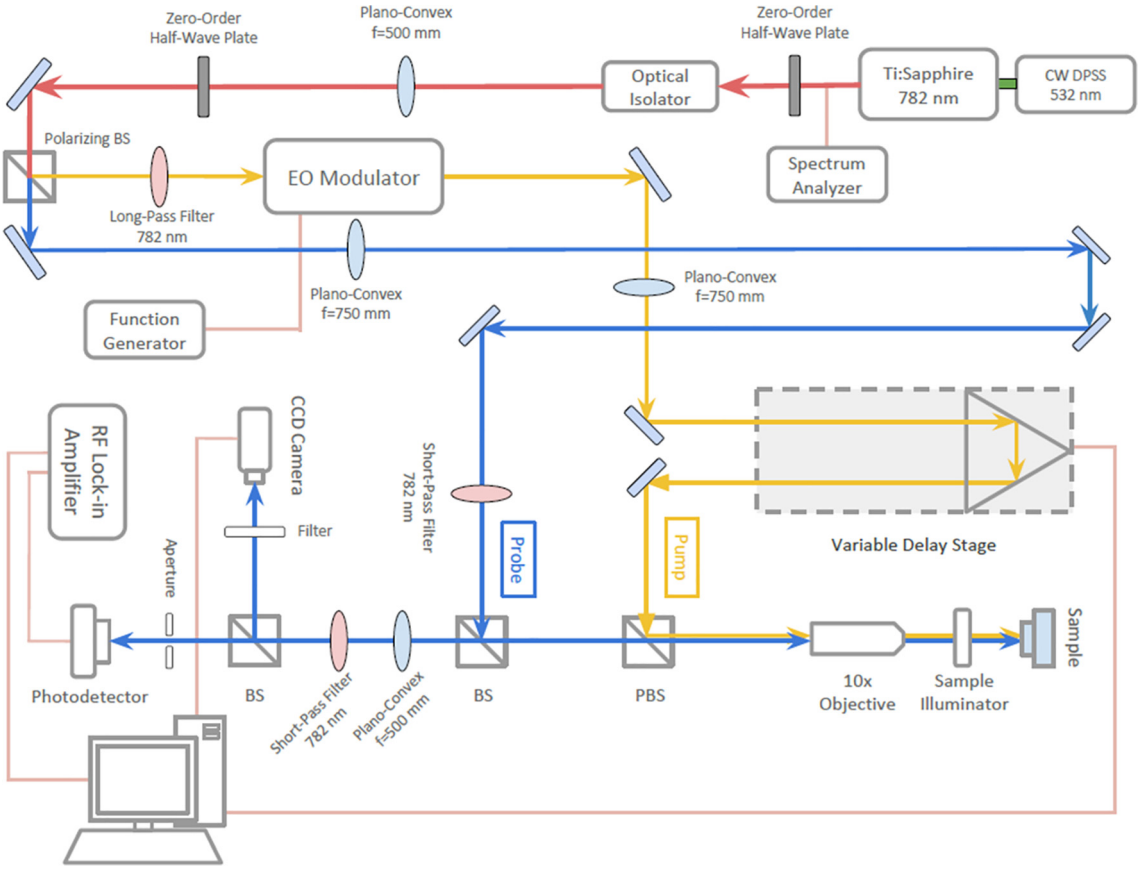

Fig. 2. TDTR experimental setup.

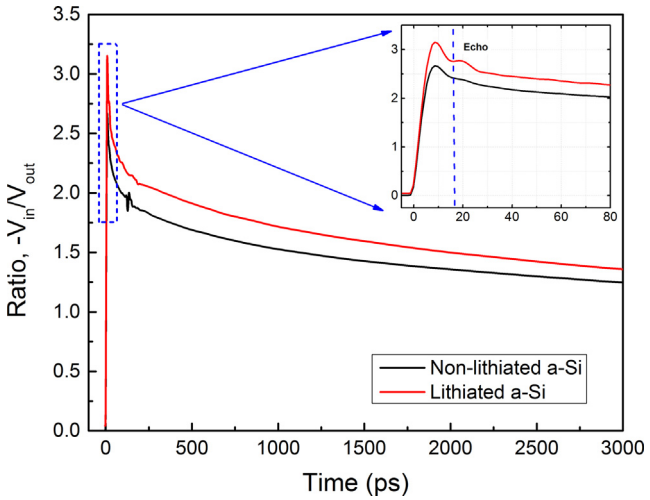

Fig. 3. Measured thermoreflectance signals for non-lithiated and lithiated Si films. The inset shows zoomed view of picosecond acoustic echo indicating Al thickness of around 60 nm.

to excite SAWs. The laser beam is focused by a cylindrical lens on the surface of the sample in the form of a straight line to form a linear source of thermo-elastic SAWs propagating along the surface of the sample by planar wave fronts. The generated laser-acoustic surface signal is detected by the sensor through a piezoelectric transducer and recorded with an oscilloscope.

The signal is measured at several distances from the source, as a result of which the phase velocity is determined and, using Fourier transform, frequency-dependent phase spectrum. This allows us to construct a phonon dispersion curve, the fitting of which with the theoretical curve gives the value of the film's Young modulus. The measurement process is fully automated and controlled from a computer.

3. Results

To determine thermal conductivity of a-Si film, the thermal conductivity of heat transducing Al layer and volumetric heat capacity of both Al and a-Si should be known. These parameters were taken from the literature and the recorded thermal reflectivity signal was then fitted using heat diffusion model [28]. Before measurements we tested our setup by measuring Al/glass sample as a reference, where Al thickness was around 60 nm and the glass was bulk sample. The thermal conductivity of glass was estimated to be around 1.3 W $m^{-1}K^{-1}$ which is very close to the accepted literature value. Fig. 4a shows measured experimental results of a-Si samples fitted by theoretical heat diffusion model (red lines). To ensure the measurement accuracy we measured at several points for both non-lithiated and lithiated samples and calculated standard deviation in measured thermal conductivity values. For the pristine (non-lithiated) a-Si thermal conductivity was around ~1.4 W $m^{-1}K^{-1}$, which is very close to the average literature value [29]. In the carried out measurements, some variation in the recorded results have been noticed. For lithiated samples, the thermal conductivity in some regions increased up to 2.2 W $m^{-1}K^{-1}$, while in other regions it remained around 1.3 W $m^{-1}K^{-1}$. The average thermal conductivity was around 2.0 ± 0.4 W $m^{-1}K^{-1}$. Such sizeable deviation is likely due to inhomogeneous in-plane and cross-plane Li^+ ions distribution in the near-surface region. Fig. 5a shows a cross-sectional SEM/FIB image of a-Si thin film anode (on rough Cu foil) experienced one lithiation/delithiation cycle. The non-uniform morphology after the first lithiation of the Si film can be observed. The film's upper part is looser and an expansion can be seen easily, while the lower part is much denser due to Li^+ ions did not reach it during first lithiation [30]. After medium degree (up to potential of 0.3 V, ~$Li_{1.7}Si$) and high degree (up to 0.05 V, ~$Li_{3.75}Si$) of lithiation, the thickness of a-Si films increased up to 650 nm and 1000 nm, respectively.

Fig. 5b demonstrates the x-ray diffraction (XRD) of the lithiated a-Si film after high degree of lithiation, where the presence of $Li_{3.75}Si$ alloy can be noticed. Further investigation will be needed to check the different levels of lithiation and also the Li^+ ions distribution in the near-surface region. At the considered level of lithiation and after only 1st lithiation, Si material did not exhibit the substantial degradation from Fig. 5a. However, an extensive delamination and cracking of Si film from the substrate happen upon cycling [17]. Such fracture can act as barriers for the heat transfer, impeding the quick reduction of the temperature in the system. Therefore, the battery cell can overheat accelerating aging of electrolyte and the entire system. In general, the insertion of Li into Si structure led to the increase of thermal transport but it is hard to isolate the contribution of Li^+ ions to the change in thermal conductivity from other possible structural mechanism.

Additionally, the studies of the Young's modulus were performed that can provide an information of mechanical strength of anode material as a function of lithiation level. Fig. 4b left shows the results of the measurement Young's modulus of a-Si anodes, depending on the degree of lithiation. The first point at 3 V refers to the as-prepared a-Si, the second point at 0.3 V corresponds to

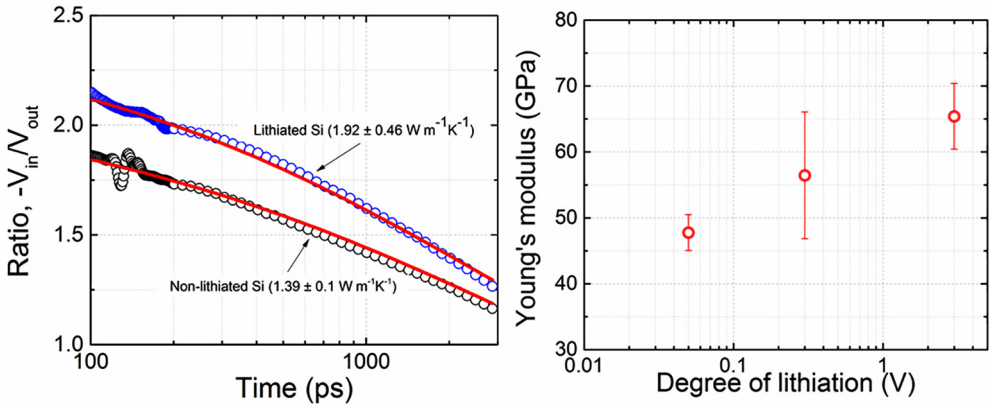

Fig. 4. (a) Measured (open dots) signals and corresponding theoretical fittings (red lines), (b) Measured values of Young's modulus of amorphous Si anodes versus degree of lithiation. (For interpretation of the references to colour in this figure legend, the reader is referred to the web version of this article.)

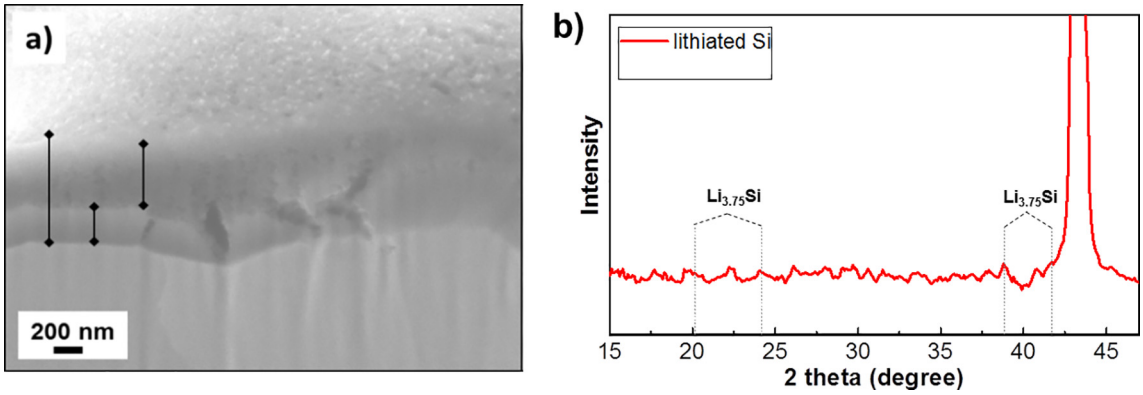

Fig. 5. (a) Post-mortem cross-sectional SEM/FIB image of Si thin film after lithiation/delithiation cycle. (b) XRD of lithiated a-Si thin film.

medium level lithiated sample and the highest lithiation of a-Si is at 0.05 V. As expected, the elastic properties of the samples deteriorate after lithiation due to the substantial volume enhancement of a-Si film [31,32] and this deterioration occurs linearly for our samples which agrees with previous studies [22].

4. Conclusion

Herein, we have observed an increase in thermal conductivity for the lithiated a-Si which is mainly due to expansion of a-Si volume (from ~330 to ~1000 nm) due to Li_xSi alloys formation and possibly due to inhomogeneous lateral lithiation of a-Si film in the near-surface region.

The values of Young's modulus decreased from 65.39 ± 4.99 to 47.75 ± 2.7 GPa, which is expected because of the a-Si volume increase as a result of Li_xSi alloy formation. As for the SAW excitation method, the measured value of the Young's modulus for the non-lithiated sample corresponded to the literature data and the standard deviation is within the acceptable range.

Thus, the obtained results may push forward to better understanding of the thermal transport and mechanical mechanisms taking place at the Li^+ ions insertion/extraction in Si anodes and, subsequently, pave the way for the ability to predict the behaviour or Si-based anodes based in the next-generation LIBs. The *in situ* time-resolved control of thermal conductivity across a-Si anode film in electrochemical cell is planned for subsequent studies.

TDTR and SAW methods have proved to be powerful tools for non-destructive optical characterization of thin films and have potential for *in situ* thermo-mechanical monitoring of battery operation. It is quite possible that the changes of the thermal conductivity of Si during lithiation can provide the access to the important information of the electrode such as state of charge (SOC).

Declaration of Competing Interest

The authors declare that they have no known competing financial interests or personal relationships that could have appeared to influence the work reported in this paper.

Acknowledgements

Authors acknowledge funding from the State Targeted Programs BR05236454 and BR05236524, and research grant AP05130446 from the Ministry of Education and Science of the Republic of Kazakhstan and the Nazarbayev University Faculty Development Competitive Research Grants 110119FD4501 and 110119FD4504.

References

[1] P. Simon, Y. Gogotsi, B. Dunn, Science 343 (80) (2014) 1210–1211.
[2] M.C. Lin, M. Gong, B. Lu, Y. Wu, D.Y. Wang, M. Guan, M. Angell, C. Chen, J. Yang, B.J. Hwang, H. Dai, Nature 520 (2015) 325–328.
[3] R. Zhao, S. Zhang, J. Liu, J. Gu, J. Power Sources 299 (2015) 557–577.
[4] T.M. Bandhauer, S. Garimella, T.F. Fuller, J. Electrochem. Soc. 158 (2011) R1.
[5] R. Spotnitz, J. Franklin, J. Power Sources 113 (2003) 81–100.
[6] H. Maleki, J.R. Selman, R.B. Dinwiddie, H. Wang, J. Power Sources 94 (2001) 26–35.
[7] P. Goli, S. Legedza, A. Dhar, R. Salgado, J. Renteria, A.A. Balandin, J. Power Sources 248 (2014) 37–43.
[8] J. Cho, M.D. Losego, H.G. Zhang, H. Kim, J. Zuo, I. Petrov, D.G. Cahill, P.V. Braun, Nat. Commun. 5 (2014) 1–6.
[9] L. Song, Y. Chen, J.W. Evans, J. Electrochem. Soc. 144 (1997) 3797–3800.
[10] V. Vishwakarma, A. Jain, J. Power Sources 272 (2014) 378–385.
[11] Y. Yang, X. Huang, Z. Cao, G. Chen, Nano Energy 22 (2016) 301–309.
[12] C.J. Wen, R.A. Huggins, J. Solid State Chem. 278 (1981) 271–278.
[13] H. Wu, Y. Cui, Nano Today 7 (2012) 414–429.
[14] M.N. Obrovac, L. Christensen, Electrochem. Solid-State Lett. 7 (2004) A93–A96.
[15] J. Graetz, C.C. Ahn, R. Yazami, B. Fultz, Electrochem. Solid State Lett. 6 (2003) A194–A197.
[16] V. Poborchii, N. Uchida, Y. Miyazaki, T. Tada, P.I. Geshev, Z.N. Utegulov, A. Volkov, Int. J. Heat Mass Transf. 123 (2018) 137–142.
[17] A. Mukanova, A. Jetybayeva, S.-T. Myung, S.-S. Kim, Z. Bakenov, Mater. Today Energy 9 (2018) 49–66.
[18] J.H. Ryu, J.W. Kim, Y.-E. Sung, S.M. Oh, Electrochem. Solid-State Lett. 7 (2004) A306.
[19] L.Y. Beaulieu, K.W. Eberman, R.L. Turner, L.J. Krause, J.R. Dahn, Electrochemic. Solid-State Lett 4 (2001) A137–A140.
[20] Z. Xie, Z. Ma, Y. Wang, Y. Zhou, C. Lu, RSC Adv. 6 (2016) 22383–22388.
[21] D. Wang, D. Wang, Y. Zou, C. Lu, Z. Ma, Acta Mech. 229 (2018) 3293–3303.
[22] V.B. Shenoy, P. Johari, Y. Qi, J. Power Sources 195 (2010) 6825–6830.
[23] R. Deshpande, Y. Qi, Y.T. Cheng, J. Electrochem. Soc. 157 (2010) A967–A971.
[24] T.D. Hatchard, J.R. Dahn, J. Electrochem. Soc. 151 (2004) A838.
[25] D.G. Cahill, Rev. Sci. Instrum. 75 (2004) 5119–5122.
[26] A. Abdullaev, B. Muminov, J. O'Connel, V. Skuratov, V. C. Chauhan, M. Khafizov, Z. N. Utegulov, Jour. Appl. Phys., Thermal transport across nanoscale damage profile in sapphire irradiated by swift heavy ions (2019) in press. http://doi.org/10.1063/1.5126413.
[27] D. Schneider, B. Schultrich, Surf. Coat. Technol. 98 (1998) 962–970.
[28] D.G. Cahill, P.V. Braun, G. Chen, D.R. Clarke, S. Fan, K.E. Goodson, P. Keblinski, W.P. King, G.D. Mahan, A. Majumdar, H.J. Maris, S.R. Phillpot, E. Pop, L. Shi, Appl. Phys. Rev. 1 (2014) 011305.
[29] S. Moon, M. Hatano, M. Lee, C.P. Grigoropoulos, Int. J. Heat Mass Transf. 45 (2002) 2439–2447.
[30] A. Mukanova, A. Serikkazyyeva, A. Nurpeissova, S.-S. Kim, M. Myronov, Z. Bakenov, Electrochim. Acta 330 (2020) 135179.
[31] H. Wu, G. Chan, J.W. Choi, I. Ryu, Y. Yao, M.T. McDowell, S.W. Lee, A. Jackson, Y. Yang, L. Hu, Y. Cui, Nat. Nanotechnol. 7 (2012) 310–315.
[32] M. Ge, Y. Lu, P. Ercius, J. Rong, X. Fang, M. Mecklenburg, C. Zhou, Nano Lett. 14 (2014) 261–268.
[33] V.C. Chauhan, A. Abdullaev, Z. Utegulov, J. O'Connel, V. Skuratov, M. Khafizov, AIP Adv. 10 (2020.) 015304.